Chapter 2
Nanotechnology Applications in Petroleum Refining

Ubong J. Etim, Peng Bai, and Zifeng Yan

Abstract Nanotechnology has successfully gained applications in many areas of life, thereby seen as the modern way of creating products, which results in high efficiency of use. In the petroleum processing industries, this revolution is no exception. The efficiency of a number of conversion processes improves upon application of materials with the nanometer scale dimension, which is caused by improvements and developments of better material properties as the particle size decreases. In this chapter, the applications of nanotechnology through nanocatalysis in petro-refining processes are highlighted. This is exemplified by discussing the applications of nanotechnology in several typical petroleum refining processes, including catalytic cracking, oxidative dehydrogenation of alkanes, and desulfurization. Other processes for the production of clean fuels are also briefly reviewed. The key benefits of "nano-tech" application in catalysis are based on the exposure of a large surface area for reaction, thereby reducing the tendencies to adverse and side reactions. The desire for an improved catalyst with high activity, low deactivation, and low coke formation to meet the growing demand for chemicals and fuels necessitates the increasing exploitation of nanoparticles as catalysts.

Keywords Nanotechnology • Nanomaterial • Nanocatalysis • Petroleum processing

1 Introduction

The quest for exploring and improving the properties of materials at atomic scales has driven scientists to a broad field of research known as nanotechnology. Fundamentally, at the nanoscale, the properties of materials between 1 and 100 nm provide new insights into improvements of the existing materials and ways to

U.J. Etim • P. Bai (✉) • Z. Yan (✉)
State Key Laboratory of Heavy Oil Processing, China University of Petroleum, Qingdao 266580, China

PetroChina Key Laboratory of Catalysis, China University of Petroleum, Qingdao 266580, China
e-mail: baipeng@upc.edu.cn; zfyancat@upc.edu.cn

T.A. Saleh (ed.), *Nanotechnology in Oil and Gas Industries*, Topics in Mining, Metallurgy and Materials Engineering, DOI 10.1007/978-3-319-60630-9_2

designing novel ones with striking features can be successfully and effectively explored. Nanotechnology has successfully gained applications in many areas of life, resulting in improved efficiency of product creation and utilization. In the scientific world, the term "nano" is used as a prefix that means "billionth" or a factor of 10^{-9} or $1/10^{9}$. A nanometer, therefore, refers to a unit which indicates an order of spatial measurement that is one "billionth" of a meter.

Nanotechnology could be defined as the science, engineering, and application of materials at the nanoscale (i.e., at least one dimension measured in nanometer) (Zhou 2007). The nanoscale means dimensions in the order of 100 nm or less. With the increased sensitivity of analytical tools at the nanometer levels, nanoscience has thus brought one of the most incredible and remarkable revolutions into the world of material science, enabling diverse applications. The first mention of the idea and concept of nanoscience and nanotechnology is credited to a physicist, Richard Feynman, in 1959 during a talk to the American Physical Society, where he described the process in which scientist could be able to manipulate and control materials at the nanoscale. The talk titled "*There is plenty of room at the bottom*" allows humanity to benefit from the implication of materials to obtain miniaturization for applications of the previous technologies.

The impacts of nanotechnology in the society have been unambiguously and overwhelmingly felt in many areas through improved efficiency and high-quality products developed at reduced overhead cost, which increases demand. Thus, nanotechnology can be considered fundamental to the modern ways of life. Improved and efficient products which span all sectors of the society are immediate consequences of the intimate integration of the so-called nano-tech. Presently, nanotechnology is applied to all areas of life, and its applications are exploited in a number of industries, including electronics, materials and manufacturing, aerospace, photography, construction, chemicals as well as petroleum refineries. The oil and gas industries, from upstream through the midstream to downstream have gone through stages where chemical processes are facilitated because of the relevancy of employing materials with unique size-dependent properties.

1.1 Nanosize

Just how small is the *nanosize*? "Nano" is about as small as it gets in the world of regular physical, materials, and biological sciences (Lindsay 2009). Based on the units, things are measured in our everyday life, for instance, the diameter of a hydrogen atom is about one-tenth of a nanometer, so the nanometer scale is the smallest scale on which one might consider building blocks on a scale. Generally, atoms are smaller than a nanometer, one atom measures in the range of ~0.1–0.3 nm, depending on the type of the element. As could be seen in Fig. 2.1, several other objects exist at the nanometer scale. Examples include viruses (30–50 nm), DNA (2 nm), buckyballs (1 nm in diameter), carbon nanotubes (~1 nm in diameter), and many catalysts used in the production of fuels and petrochemicals are based on nanoparticles. The thickness of a sheet of paper is

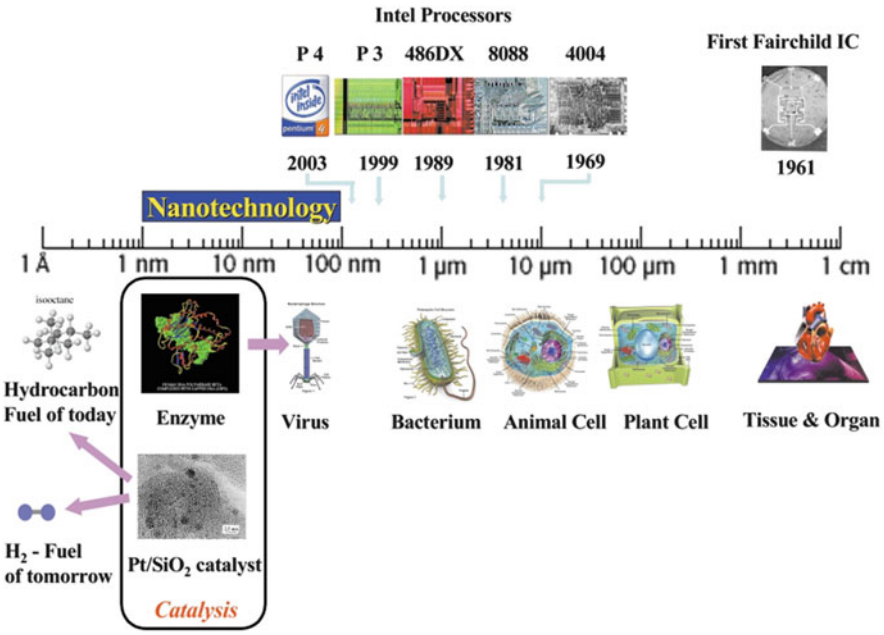

Fig. 2.1 Some nanometer-sized materials. Adapted from Grunes et al. (2003), with permission of the Royal Society of Chemistry

about 100,000 nm and the human hair is about 50,000–100,000 nm in diameter (Grunes et al. 2003). Objects and dimensions that are this small are difficult to measure with the conventional instruments and require special tools for analysis. So, the sensitivity of measurement is enhanced using powerful microscopic tools that permit the use of unique methods to allow for the visualization of surface features on the atomic scale, such as atomic force microscopy (AFM), scanning electron microscopy (SEM), transmission electron microscopy (TEM), and scanning tunneling microscopy (STM). These characterization tools have been frequently used to examine the nanostructure of model catalyst systems. Using STM, for example, it becomes possible to explain why doping Ni catalysts used for the steam reforming of methane with a small amount of gold reduces the tendency of such catalysts to deactivate because of carbon deposition (Besenbacher et al. 1998).

1.2 Nanomaterials

Nanomaterials possess unique properties derived from features present in them that are measurable on the nanometer scale. Examples of nanomaterials in use in modern industrial applications include carbon materials, metal oxides, and zeolites.

The preparation of materials at the nanoscale is feasible through careful design and controlled synthesis procedures. Generally, nanomaterials can be synthesized by two widely known methods, either by bottom-up or top-down approach. The bottom-up approach involves the formation of nanomaterials by reaction and assembly of the reactants in the presence or absence of structure directing agents (SDA). In the top-down approach, the bulk materials are broken down to smaller particle size by mechanical, thermal, or chemical methods. The former has the advantage of precise control of the particle size; however, the use of expensive precursors and surfactant increases cost. The latter has the disadvantage of nonuniform particle size. Faujasite zeolite nanosheets, for example, are synthesized by controlling the pore structure using SDA and crystallization temperature that allow for the formation of zeolite particles with interstitial pores between the nanosheet assemblies (Inayat et al. 2012; Mehlhorn et al. 2014; Yutthalekha et al. 2016). The most important property to optimize during the synthesis of nanomaterials is the surface area. The shape, size, and composition of the surface need to be controlled as well. These properties are of basic importance in applications involving catalysis because they are the determinants of catalyst activity and stability. Often, the surface area increases with a decrease in the dimension of a material. Thus, as the material size decreases, a greater portion of the atoms are found at the surface compared to the bulk material. Because growth and catalytic chemical reactions occur at materials surfaces, a given mass of nanomaterial reacts more compared to the same mass of bulk material. Additionally, materials that are inert in their bulk form are reactive when existing in nanoscale. Nanomaterials are expected to have a much greater surface area per unit volume compared with larger particles. This property makes them more chemically reactive because atoms at the surface of some materials do not have covalent bonds as they are in an energetically unstable state. Since more atoms located at the surface are in energetically unstable states, nanomaterials are more reactive compared to the bulk materials.

1.3 Nanoparticles

Nanoparticles in principle have sizes ranging between 1 and 100 nm (Rao et al. 2002). Their physical and chemical properties are intermediate those of the atom of an element and the bulk material. The beneficial aspect of this class of materials as compared with their bulk (microparticles greater than 1 μm) is often size-dependency of functions. As the size decreases and approaches the nanoscale, new and fascinating functional properties develop and become significant, such as color change and phase transformation. For example, the unique physical properties of nanoparticles allow high absorption of radiation in photovoltaic cells that are composed of nanoparticles than does in thin films of continuous sheets. Other examples of size-dependent property changes could be seen in quantum confinement in semiconductor particles, surface plasmon resonance in some metal particles, and in chemical reactivity that is utilized for image formation

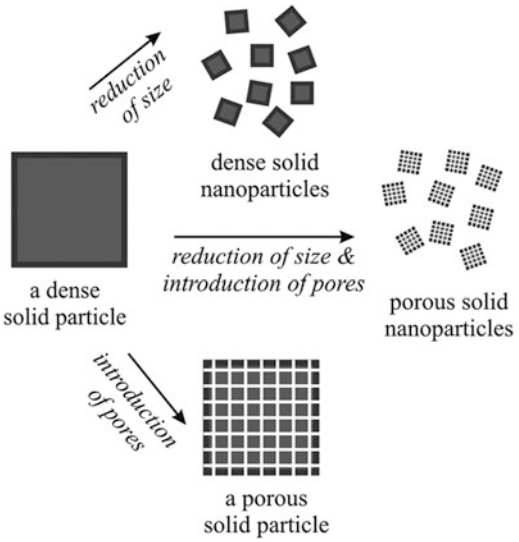

Fig. 2.2 Schematic illustration of the ways to increase the surface area of dense solids. Adapted with permission from Valtchev and Tosheva (2013). Copyright (2013) American Chemical Society

in photography (Lindsay 2009). Increasing the number of surface atoms in a material often increases surface-to-volume ratio and chemical potentials in the material (Zhou et al. 2009). The number of surface atoms in solid materials can be increased by (1) decreasing the size of bulk particles or (2) creating open pore network within the bulk of the material as illustrated in Fig. 2.2 (Valtchev and Tosheva 2013). Another unique method is to synthesize nanosized particles containing accessible and uniform nanopores. The size of nanoparticles is very instrumental in determining chemical properties. In catalysis, nanoparticles or nanomaterials play a vital role in improving chemical transformations.

1.4 Nanocomposites

A nanocomposite is a multiphase solid material in which at least one of the phases has one, two, or three dimensions of less than 100 nm. In other words, a nanocomposite material is composed of a bulk matrix and at least one nano-dimensional phase with properties different from those of the matrix. The properties of a nanocomposite differ considerably from those of the constituent and/or conventional composite materials due to dissimilarities in structure and chemistry, the exceptionally high surface-to-volume ratio of the reinforcing phase and/or its exceptionally high aspect ratio. A reinforcement surface area indicates that a small amount of nanoscale reinforcement has an observable effect on the macro-scale properties of the nanocomposite. As an example, loading carbon nanotubes enhances the electrical and thermal conductivity of a conductor bulk material. Also, some nanomaterials result in enhancing optical, dielectric, and mechanical

characters and heat resistance. Examples of nanocomposites include porous media, colloids, gels, and copolymers. The mechanical, electrical, thermal, optical, electrochemical, and/or catalytic properties of a nanocomposite differ markedly from those of the individual component materials. Size limits for these effects have been proposed: size <5 nm finds applications in catalysis, <20 nm for making a hard magnetic nanomaterials soft, <50 nm for refractive index changes, as well as <100 nm to achieve super magnetism, mechanical strengthening or restricting matrix dislocation movement (Kamigaito 1991).

2 Nanocatalysis

The application of nanotechnology in petroleum refining is mainly driven by the creation of nanocatalysts that have led to improvement in the fields of both homogeneous and heterogeneous catalysis. Nanoparticles are important catalysts for petroleum processing and energy conversion. The performance of a catalyst is sensitive to particle size because the surface structure and electronic properties can change greatly with size (Zhou et al. 2009; Bell 2003). For example, the heat of adsorption for CO and the activation energy for CO dissociation both change with increasing the size of Ni particles, consequently, affecting the performance of Ni nanoparticles in the Fischer–Tropsch synthesis of hydrocarbons from synthesis gas (Bell 2003). Reducing the particle size of porous materials to nano-dimensions allows for the optimization of their applications in catalysis. Nanoporous materials show improved catalytic activity in diffusion-limited reactions, and manipulation of nanocrystalline suspensions using colloidal chemistry approach results in the preparation of 2D and 3D microporous materials with adjusted characteristics for catalytic reactions (Valtchev and Tosheva 2013).

Nanocatalysis involves the synthesis and characterization of supramolecular materials at the nanometer level and their controlled applications (Schlögl and Abd Hamid 2004). It differs from conventional catalysis since the materials are explicitly designed to a length scale much larger than that of a single active site. It has been demonstrated in various reactions that the use of nanocatalyst can decrease the energy requirements in chemical processes, resulting in a greener chemical industry. The contribution of nanoscience and nanotechnology may have been seen as a springing science in catalysis; however, it will be of beneficial interest to clarify that the selectivity principles by which heterogeneous catalytic reactions proceed rely exclusively on nanocatalysis, and the use of small particles in technical catalysis has been operated for ages (Schlögl and Abd Hamid 2004).

Nanoporous materials are fundamental to the modern petroleum refining and the petrochemical industry. Zeolites, for instance, are employed as key catalysts in petroleum refining. Zeolites are crystalline aluminosilicate materials with well-defined pore connection dependent on the particular topology. There are about 230 zeolite framework types ("Database of Zeolite Structures, http://www.iza-structure.org/databases/") of which the commonest ones employed in large

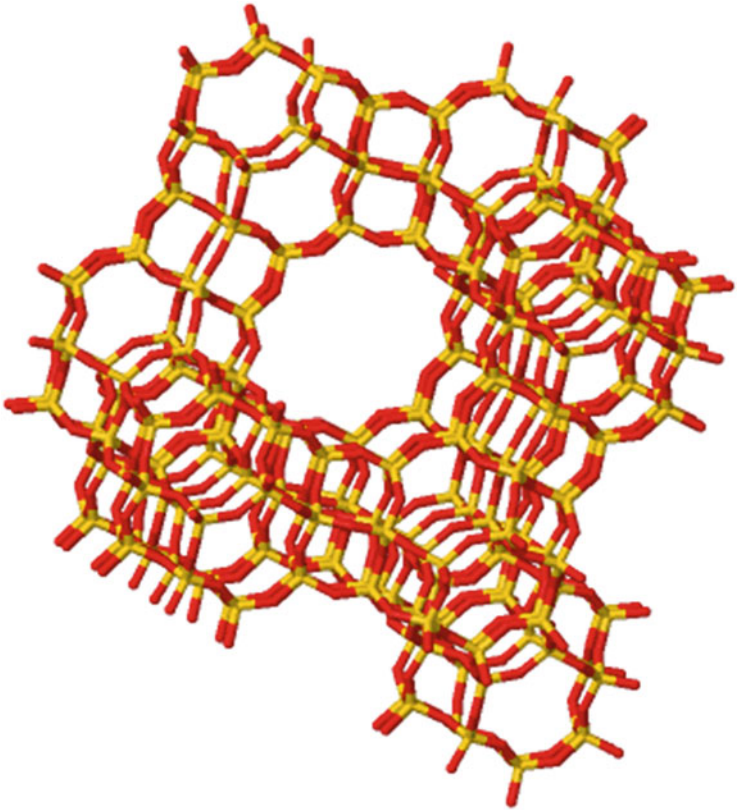

Fig. 2.3 Structure of zeolite Y (FAU). Constructed from ("Database of Zeolite Structures, http://www.iza-structure.org/databases/")

quantities in the petroleum refining and the petrochemical industry are zeolite Y and ZSM-5 of FAU and MFI topologies as in Figs. 2.3 and 2.4, respectively. Of special note is that these zeolites consist in nano-pores that allow for molecular sieving functionalities in them as shown in Fig. 2.5. So far, their excellent shape selective properties position them as one of the most important heterogeneous catalysts practically in use.

The relevant nano-pore sizes (0.74–1.2 nm in zeolite Y and 0.54–1.0 nm in ZSM-5) afford these zeolites the ability to screen heavier hydrocarbon molecules, allowing only those with a diameter less than or equal to their pore size to pass through. For more than five decades, zeolites have contributed immensely to the growth of the petroleum industry, being a catalyst for the transformation of less valued crude oil fractions to more valued and desirable products by a process known as fluid catalytic cracking (FCC). Although zeolites contain inherent nanosized pores that classify them as nanomaterials, they are usually of micrometer particle size. Controlling the synthesis conditions of the conventional micrometer-

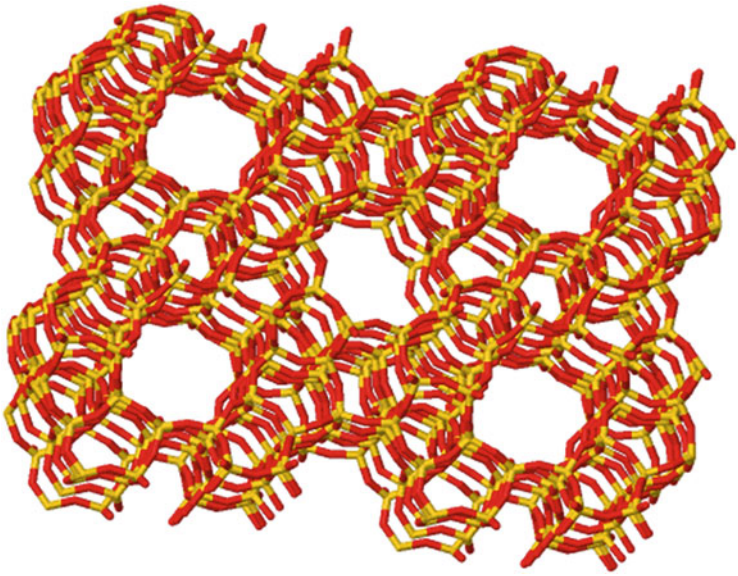

Fig. 2.4 Structure of zeolite ZSM-5 (MFI). Constructed from ("Database of Zeolite Structures, http://www.iza-structure.org/databases/")

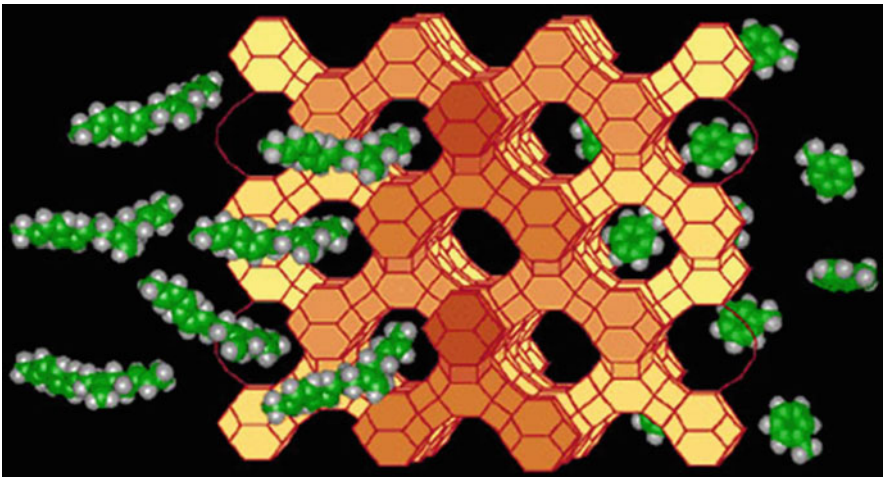

Fig. 2.5 Molecules diffusion through the zeolite Y pore (~7.4 Å). Adapted from ("Database of Zeolite Structures, http://www.iza-structure.org/databases/")

sized zeolite could result in entirely nanosized zeolites such as nanosheets. For practical applications in catalytic reactions, it is important to understand the differences between the nanocrystals and microcrystal zeolites. The nanocrystal zeolites exhibit high external surface area, which is advantageous for processing

bulky molecule that cannot penetrate through the small pores and channels of zeolites. In addition, they have shorter diffusion path lengths than the conventional micrometer-sized zeolite (Farcasiu and Degnan 1988; Weisz 1995).

2.1 Supported Metal Catalysis

2.1.1 Catalyst Support

The advances in the synthesis of materials for improved catalytic performance of various reactions have led to exciting strategies for creating catalyst particles that are of very small size. In most of the applications, these catalysts are sat on porous metal oxide supports, which have diameters in orders of a nanometer. This strategy contributes to the production of nanometer length scale catalysts that are very active and stable under various high reaction severities. Among the widely used support materials for catalyst fabrication, alumina and silica have received considerably most applications for reasons pertaining to cost-effectiveness and excellent physicochemical properties as catalyst supports. Aluminas are widely employed as standard supports for many metal and sulfide catalysts at the industrial scale. For catalysts requiring relatively low reaction temperature (less than 500°C), such as for hydrogenation using platinum, palladium, or metal sulfides as active phase, high surface area alumina can be used. For low-temperature reactions, such as partial oxidation reactions, transition aluminas are preferable. Stabilized aluminas with silica or alkali, alkali-earth, or rare earth cations (K^+, Ca^{2+}, La^{3+}, etc.) are extensively used for reactions requiring medium to high temperatures. An example is the case of some endothermic reactions such as steam reforming or partial oxidation reactions using platinum or rhodium catalysts. Silicas possess excellent mechanical and thermal stabilities and are also widely used as supports for industrial applications. Nickel and copper catalysts supported on silica are frequently used for hydrogenation reactions. In some other cases, silicas are used as stabilizers as a very little amount is required.

2.1.2 Particle Size Effect of Metal Oxide Supports

The influence of crystalline structure or particle size on the solid-state chemistry of materials, including metal oxides used as catalyst supports has received great attention recently. It has long been conceived but came to limelight at the birth of nanoscience and nanotechnology. Practically, nanostructured catalysts are more stable materials in comparison to its bulk counterparts for the reason that the surface-free energy predominates in the bulk. This was first reported for γ-Al_2O_3 with respect to corundum α-Al_2O_3 (McHale et al. 1997) and for other polymorphic systems such as anatase-TiO_2 with respect to rutile (Zhang et al. 2009) as well as tetragonal ZrO_2 in comparison to monoclinic zirconia (Zhang et al. 2006).

Therefore, the easy formation and stabilities of γ-Al_2O_3, anatase TiO_2, and tetragonal ZrO_2 at room temperature are because of their existence in the form of nanoparticles (Busca 2014). An unpromoted, size-selected Ag_3 clusters and ~3.5 nm Ag nanoparticles on alumina supports can catalyze direct propylene epoxidation with only a negligible amount of carbon dioxide formation and with high activity at low temperatures (Lei et al. 2010), whereas bulk Ag catalyst produces substantial amount of carbon dioxide. Density functional calculations show that, relative to extended silver surfaces, oxidized silver trimers nanoclusters are more active and selective for epoxidation reaction because of the open-shell nature of their electronic structure (Lei et al. 2010). Valence electrons in bulk metals form continuous bands, and upon reduction of the bulk material in a certain direction down to the nanometer scale, the motion of electrons in this direction is subject to confinement (Yang et al. 2015; Valden et al. 1998). In this regard, compared to bulk metals, nanoparticles exhibit much larger total exposed surface areas and various combinations of surface structures, and the electronic confinement effects within nanoparticles lead to major changes in the electronic structure (Valden et al. 1998; Haruta and Daté 2001). This raises the possibility of tuning the catalytic process. In this way, nanotechnology could provide an effective means through which the surface structure and electronic properties of supported nanocatalysts can be effectively controlled without changing their composition. A very small crystal size of the nanocrystalline zeolite contributes favorably to both the formation of a high external surface area, with no steric constraints, and to a faster diffusion of reactant molecules to the acid sites located within the zeolite micropores (Serrano et al. 2010). This feature leads to catalytic performance improvement. It is therefore clear that the activity and selectivity of catalyst nanoparticles are strongly dependent on their size and shape as well as surface and electronic structures.

Particle size reduction of the active metal offers an invaluable benefit to energy cost reduction. Au nanoparticles having dimensions less than 10 nm are often used for various applications including catalysis. In catalysis, selective oxidation of ethanol in oxygen catalyzed by SiO_2 supported Au shows an improved activity at a lower temperature than does the bulk Au catalyst (Zheng and Stucky 2006). This behavior, besides improved catalytic activity, demonstrates energy conservation that comes with smaller particle size catalyst. The size of Co particles plays a key role in determining its selectivity performance. Co nanoparticles with a mean diameter of 6–10 nm can improve the selectivity of C_{5+} hydrocarbons than the bulk Co (Bezemer et al. 2006). In the following sections, selected examples of petro-refining/chemical processes where nanotechnology finds immense applications are discussed.

3 Petroleum Refining Processes

3.1 Catalytic Cracking

Catalytic cracking occurs on solid acids catalysts. Its development in the late 1930s brought a revolution into the petroleum industry that was previously relied entirely on thermal cracking. The cracking catalysts are usually crystalline aluminosilicate solids with acid sites strong enough to cause the scission of carbon–carbon bond in hydrocarbon molecules. Unlike thermal cracking, the use of powder catalysts provides alternative routes for cracking by lowering the activation energy for the reaction. One of the areas where the application of nanoscience has a success story is the petroleum refining. As mentioned earlier, the use of zeolite catalyst in the FCC for the conversion of heavy crude oil fractions has been an important revolution in the petroleum industries since the 1960s, and its significant contributions are continuously felt hitherto. As of today, over seven million barrel of petroleum products and chemical are annually produced using the zeolite catalyst (Zhou 2007).

3.1.1 Nanozeolite

Crystalline zeolites have 3D networks of well-defined micropores (<1.2 nm). With these pore constraints, only molecules of comparable or size less than the pore aperture can access the active sites. Catalytic reactions are therefore restricted to the molecules having a diameter below the pore constraints. Thus, larger feed molecules are then crack on the external surface of the zeolite. The use of nanosized zeolite could overcome this limitation because as the ratio of external to internal number of atoms increases when the particle size decreases, the zeolite nanocrystals present a large external surface area and high surface activity (Vuong et al. 2010). The improved surface area exposes move acidic sites for catalytic reactions. This increases catalytic performance due to higher accessibility to active sites. Decreasing the zeolite crystallite size has been demonstrated to increase the conversion and the selectivity of gas oil (Rajagopalan et al. 1986). Compared with micron-sized, nanosized zeolites exhibit a higher activity, lower coking activity and longer life in many reactions. One of the pioneer studies that demonstrate the influence of zeolite crystal size on catalytic cracking was published in 1986 (Rajagopalan et al. 1986). NaY zeolite crystals size ranging from 60 nm to 0.65 μm was employed for catalytic conversion of gas oil in the FCC reaction. The catalyst containing the smallest particles exhibited improved activity and selectivity to gasoline and light cycle oil (LCO) as in Fig. 2.6a, b. These improved selectivities were attributed to the decreased diffusion resistance to the gas oil and produced gasoline in the nanosized zeolite. With nanozeolite, the conversion of hydrocarbons can be greatly improved. Vuong et al. (2010) synthesized a series of zeolite Y nanocrystals and compared their catalytic activity in a standard gas oil cracking test. It was found that small

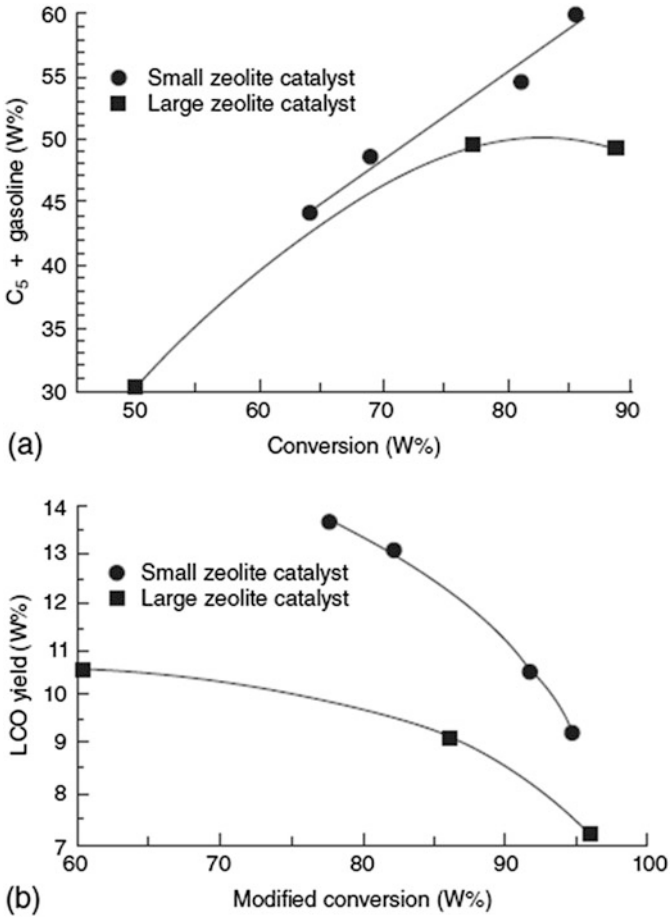

Fig. 2.6 Selectivity of heat-treated zeolite particles (2 h at 538°C) to (**a**) gasoline and (**b**) light cycle oil, LCO catalysts on west Texas heavy oil feed. Adapted from Rajagopalan et al. (1986) with permission from Elsevier. Copyright 1986 Elsevier publishers

nanosized zeolite (25, 40, and 100 nm)-based FCC catalysts exhibited higher catalytic activities compared to larger ones as illustrated in Fig. 2.7. A correlation is between gasoline selectivity in FCC feedstock conversion and zeolite particle size. This performance of zeolite catalysts followed the trend as: FCC-100 < FCC-40 < FCC-25, which can be explained by the cracking of FCC feed on the external surface of zeolite crystals.

The intrinsic properties of a catalyst can be modified by reducing the crystallite size. Nanosized ZSM-2 (~100 nm) has been recently prepared (Covarrubias et al. 2009). This type of zeolite possesses improved acidity, high surface area and maintains the structural stability that makes it highly attractive for catalytic applications. The nanosized ZSM-2 zeolite offers as an excellent catalyst support for

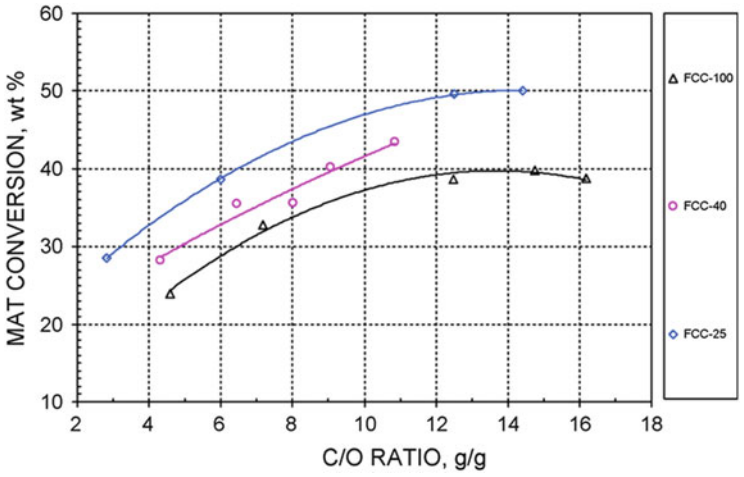

Fig. 2.7 MAT conversion curve for nanozeolites-based FCC catalyst. Adapted from Vuong et al. (2010) with permission from Elsevier. Copyright 2010 Elsevier publishers

metallocene polymerization. A nanoporous aluminosilicate (MMZ_{USY}) obtained from USY zeolite exhibits high thermal stability and accessibility for oil molecules in the conversion of bio-oil. When compared with MCM-41, the MMZ_{USY} showed excellent catalytic activity and selectivity due to improved surface acidity (Park et al. 2008). Catalytic cracking activity on the external surface of nanozeolites of FAU (zeolite Y) and MFI-type (ZSM-5) was evaluated in 1,3,5-triisopropylbenzene conversion and compared with conventional micron-sized zeolite Y and ZSM-5 crystals used as reference samples. Smaller crystal catalysts showed higher activities and an increase in conversion with the time of reaction. The conversion was high for zeolite Y, as it is related to high amounts of surface acid sites with respect to ZSM-5 (Morales-Pacheco et al. 2011). Nanosized zeolite Y crystals are employed in the selective catalytic reduction of NO_2 with urea (Li et al. 2005). The reaction rate is significantly higher than that of commercial FAU-type zeolite. The performance of nanosized crystallites when compared with that of commercial micrometer-sized zeolite Y is attributed to the larger external surface of zeolite nanocrystals rich in silanols, and extra-framework Al is found to be responsible for the higher reaction rate. Additionally, a decrease in the formation of undesired products like biuret and cyanuric acid is observed on the nanosized catalyst.

Light olefins, usually produced by the thermal cracking of naphtha, are an invaluable product of the petroleum industry and an important raw material for the petrochemical industry. Presently, an alternative method for producing light olefins in large quantities is by catalytic processes. An example is the use of methane as a source of methanol followed by methanol-to-olefin (MTO) reaction. The most often used catalysts for this reaction are ZSM-5 and SAPO-34. SAPO-34 shows higher selectivity to light olefins; however, it is rapidly deactivated due to coke deposition. A decrease in the crystal size of SAPO-34 is expected to reduce the

coke formation and thus increase the effectiveness factor (Valtchev and Tosheva 2013). Comparing the catalytic properties of nano- and micrometer-sized SAPO-34 crystals in the MTO reaction, the nanosized catalysts exhibit a longer catalyst lifetime, which is related to the enhanced diffusion and desorption of produced hydrocarbons, leaving the micropore space unblocked and thus limiting side reactions and coke formation (Hirota et al. 2010).

3.1.2 Synthesis of Nanozeolites

The synthesis of zeolite nanocrystals was somewhat challenging until recently when practical approaches have become feasible. Like the conventional micron-sized zeolites which yield particles with dimension of about 1 μm, nanocrystal zeolites are also synthesized from clear solutions under hydrothermal conditions (Persson et al. 1994; Mintova et al. 2016; Schoeman et al. 1994). Special attention is required during preparation of the initial precursor gel to favor the nucleation and crystallization processes. The number of nuclei in the homogeneous precursor solution determines the crystal size. Therefore, a system with sufficient nucleation results in very small crystals (Mintova et al. 2016). Different methods can be adopted for the synthesis of zeolite nanocrystals, namely, hydrothermal crystallization, microwave, ultrasonic, confined space, seeding and use of microreactor (Askari et al. 2013; Jo et al. 2013; Pan et al. 2009; Jacobsen et al. 2000a, b; Schmidt et al. 2000; Sun et al. 2015, Lv et al. 2013, Hu et al. 2009, Kore et al. 2014; Gao et al. 2016). Hydrothermal crystallization is the most widely employed method because of the ease to control the crystallization process. The precursor gel solution is prepared in such a way to favor the nucleation over the growth of the crystals and to limit the aggregation between the growing crystals. Furthermore, a number of other factors have to be controlled to achieve the desirable nucleation. Such factors include polymerization process during preparation of the initial precursor gel, hydrothermal treatment temperature, the amount of the metal cation in the colloidal precursor solution, and the type and concentration of SDA. In addition, alkalinity of the gel solution, crystallization time, precursor gel molar composition, and zeolite particle source affect the particle size of the synthesized zeolites and direct the growth of the crystals to the desired zeolite structure (Covarrubias et al. 2009; Sun et al. 2015; Davis et al. 2015). High supersaturation and steric stabilization of the proto-nuclei in the presence of quaternary ammonium cations play crucial roles in the formation of non-aggregated zeolite nanocrystals (Covarrubias et al. 2009).

In zeolites formation mechanism, generally, amorphous particles are initially formed and then converted into crystals with changing size. Zeolite nuclei form in the center and grow outwards until the whole amorphous particles are transformed into crystalline ones. After heating at a high temperature, larger cubic crystals are obtained (Mintova et al. 1999). However, other mechanisms of nanozeolite crystals formation have been reported in the literature. Recently, it has been shown that very small sized EMT-typed zeolite can be synthesized from template-free Na-rich precursor system (Ng et al. 2012a, b). The resulting nanosized zeolite which exhibited a size of 15 × 4 nm along the a and c directions, respectively, was

possible due to the control of the polymerization process during the preparation of the initial suspension (Ng et al. 2012a, b) and the low-temperature hydrothermal treatment that limited the growth of the crystals and inhibited competitive zeolite structures. Hierarchical beta nanozeolites were synthesized from protozeolite seeds in the presence of an organosilane as a precursor. It was found that zeolite crystallization proceeded through a condensed step mechanism, gradually growing from the evolved nuclei. The organosilane played important roles as a mesoporogen and a growth inhibitor. The crystal size and mesopore properties of the prepared hierarchical beta nanozeolites strongly depended on the properties of seeds (Sun et al. 2015).

3.2 *Oxidative Dehydrogenation of Alkanes*

Oxidative dehydrogenation (ODH) of propane is an attractive option for propene production. In the presence of oxygen, the thermodynamic restrictions of dehydrogenation are overcome and the exothermic character of the reaction renders it an energetically efficient process (Karakoulia et al. 2009). Vanadia nanoparticles supported on various oxides ZrO_2, Al_2O_3, MgO, SiO_2, TiO_2, CeO_2, and Nb_2O_5 are active catalysts for the ODH of alkanes to olefins (Khodakov et al. 1998; Corma et al. 1992; Wachs and Weckhuysen 1997; Khodakov et al. 1999). A recent study shows that the ODH activity per atom of exposed V decreases with increasing size of the vanadia clusters (Khodakov et al. 1999). Support surfaces that covered with small V_2O_5 clusters containing V–O–V or V==O linkages lead to high dehydrogenation rates and selectivities. The composition of the support influences the speciation of different VO_x species and V_2O_5 clusters, and thus the catalytic behavior of supported vanadia in ODH reactions (Khodakov et al. 1999). Also, the sizes of preselecting platinum clusters were demonstrated to greatly enhance ODH of propane to propylene (Vajda et al. 2009). Platinum nanoclusters stabilized on high surface area supports are 40–100 times more active for ODH of propane than previously reported for bulk platinum, in addition to exhibiting high selectivity to propylene over undesirable products. The superior performance of the nanoplatinum catalyst as revealed by quantum calculations indicates that undercoordination of the platinum atoms is responsible for the high reactivity with extended surfaces (Vajda et al. 2009). The calculated transition states and intermediates in the reaction of C_3H_8 leading to the formation of propylene on the Pt_4 cluster are shown in Fig. 2.8. The "true" barrier to breaking the first C–H bond is only 0.42 eV. The corresponding barrier referenced to gas-phase propane (the "apparent" barrier) is slightly smaller (0.18 eV); this barrier is found to be smaller (0.05 eV) when recalculated on a Pt_8 cluster. In spite of the small magnitude of the energetic barrier, this step will probably be rate-limiting because of the very large entropic loss, and consequently, lower pre-exponential factor, associated with propane adsorption at high temperatures on the clusters. The other pathways are thermodynamically downhill to the formation of propylene, which binds to Pt_4 by its π bond (Vajda et al. 2009).

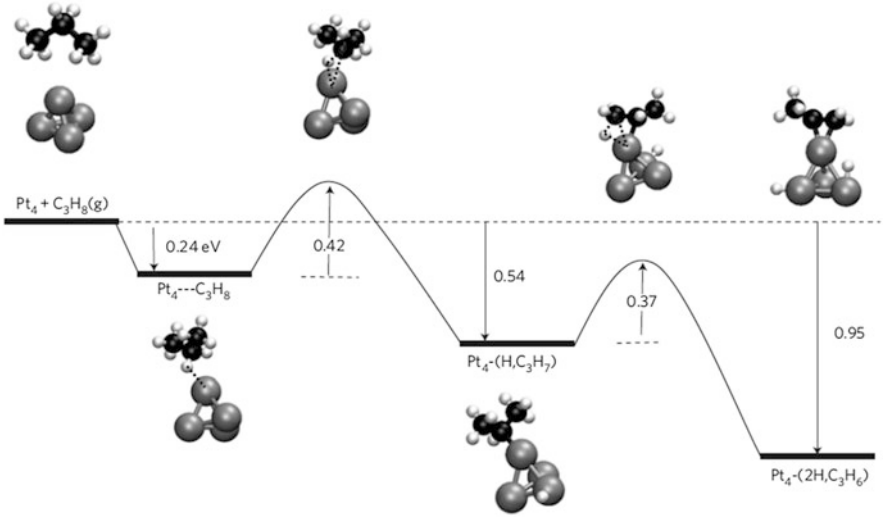

Fig. 2.8 Conversion of propane to propylene from DFT calculations for the dehydrogenation of propane on a Pt_4 cluster leading to the formation of propylene adsorbed on the cluster. Energies (in eV) of the equilibrium structures are relative to the reactants. Energy barriers for the transition state structures are relative to the preceding equilibrium structure ("true" barriers). The first barrier corresponds to breaking of the first C–H bond (on the CH_2 group) and the second barrier corresponds to breaking of the second C–H bond (on a CH_3 group). The *dotted lines* in the structures indicate partial bonds. Reprinted with permission from Macmillan Publishers Ltd. *Nature Chemistry* (Vajda et al. 2009), copyright 2009

3.3 Desulfurization of Petroleum

Due to stringent regulations by various environmental protection agencies across the world on the release of poisonous gases to the environment from petroleum exploitation, desulfurization of commercial fuels is widely practiced in order to reduce the sulfur content to less than 10 ppm in the refined petroleum products. In the upgrading of heavy oil via desulfurization, unsupported metal sulfide catalysts in its natural state are gaining serious attention. To increase the desulfurization capacity of these catalysts, the particles size need to reduce as much as possible to eliminate the introduction of toxic sulfur compounds to pre-sulfurize the hydrogenation catalysts. This simplifies the application process and improves the efficiency of the catalysts (Li and Zhu 2012). Several types of sulfur removal are carried out using metal catalysts. Catalysts based on molybdenum, cobalt, and nickel dispersed on different supports are effective catalysts for the removal of sulfur from petroleum and petroleum products (Li and Zhu 2012; Sudhakar 1998; Mohajeri et al. 2010). The composition, as well as particle size, can play an important role in the performance of the catalysts. A US patent 20100167915A1 (Mohajeri et al. 2010)

discloses that hydrodesulfurization (HDS) catalysts on nanostructured porous carbon supports are excellent for desulfurization of hydrocarbon feedstocks. A nanocomposite based on anatase-vanadium-polyphosphomolybdate ((TiO_2)/$(Bu_4N)_4H[PMo_{10}V_2O_{40}]$) shows a good capacity to oxidatively desulfurize a simulated gas oil. The nano layer of the anatase phase with a particle size of 20 nm shows a high S conversion (more than 98%) (Rezvani et al. 2014). The high oxidative desulfurization (ODS) of gas oil proves an efficient, convenient, and a practical method for scavenging sulfur compounds with this nanocomposite material. Fe@Si–$PMo_{10}V_2$ nanostructured support as a catalyst for the ODS process selectively oxidizes sulfides to the corresponding sulfoxides and sulfones under mild reaction conditions. The catalyst also exhibits excellent activity to remove sulfur contents in model oil and shows a high potential as an effective catalyst for deep desulfurization of diesel. The presence of other compounds such as nitrogen and aromatic compounds can affect ODS conversion. An important characteristic of this nanocatalyst is its reusability after at least three ODS cycles with a good catalytic activity (Rafiee and Rezaei 2016). Reusability of the catalyst is an important consideration in the design of a catalyst for industrial applications. Silver supported on mesoporous silica nanoparticles exhibits excellent regeneration stability and maintains high activity up to six cycles (Hauser et al. 2016). This is due to the reduction of silver ions to silver nanoparticles within the mesochannels of the extra-framework aluminum. The good behavior of hematite (Fe_2O_3) nanoparticles for thiophene decomposition in desulfurization reaction is a result of the unique properties of the catalyst (Khalil et al. 2015). Among other factors, the size of the hematite nanocatalyst influences the ability of the catalyst to decompose thiophene. The catalytic performance increases with an increase in reaction temperature and the amount of the catalyst but decreases with the particle size and the presence of hydrogen donor. Hydrogen donor covers the surface of the catalyst and blocks the active sites. In this reaction, the catalytic process involves a cyclic phase transformation of some of the hematite to magnetite (Fe_3O_4) as thiophene is oxidatively decomposed into its products and reoxidation of magnetite to hematite in the presence of water as the source of active oxygen (Khalil et al. 2015). Recently, carbon materials have become excellent supports for various catalysts in different desulfurization reactions (Mohammed et al. 2017; Guo et al. 2017). Nanocatalyst composite structure was prepared on various carbon nanotube supports and the formation of network structure between metal catalysts and CNTs was observed (Mohammed et al. 2017). These supports enable the homogeneous spreading of the active CoMo particles within the bulk of CNTs. Experiments using these nanocatalysts reveal better results than the conventional catalyst ($CoMo/Al_2O_3$) in the removal of sulfur from gas oil. An improvement of about 10% in HDS over conventional catalyst was obtained after 10 h under conditions: 280°C of reactor temperature, 10 bar of system pressure, and 2 h^{-1} of space velocity of gas oil, which were optimum conditions to remove sulfur from the gas oil (Mohammed et al. 2017). In an in situ experiment for upgrading heavy oil, different carbon

nanomaterials were utilized as catalysts in the HDS reaction with thiophene as a sulfur-containing model compound. The carbon nanocatalysts possessed an ultrahigh specific surface area and a good degree of graphitization. It was found that the graphitization degree of the carbon-based nanocatalysts is of great importance in the HDS reaction, contributing to catalytic activity. The performance of the carbon-based nanomaterials demonstrates the potential application of carbon nanomaterials as metal-free catalysts in in situ upgrading and recovery of heavy crude oil, which will contribute to a more sustainable chemistry in terms of production and refining of heavy crude oils (Guo et al. 2017).

Synergism of nanosized materials improves stability and recycling of catalysts for reusability (Hauser et al. 2016). Zeolites as supports for desulfurization catalysts synergistically contribute to excellent activities of the catalysts. Crystalline mordenite nanofibers support with a bundle structure containing parallel mesopore channels were tested for sulfur removal in HDS. Cobalt and molybdenum (CoMo) species were introduced into the mesopores and micropores of nano-bundles mordenite (NB-MOR). The NB-MOR supported CoMo catalyst (CoMo/NB-MOR) exhibited an unprecedented high activity (99.1%) as well as very good catalyst life in the HDS of 4,6-dimethyldibenzothiophene and diesel compared with a conventional γ-Al_2O_3 supported CoMo catalyst (61.5%). The spillover hydrogen formed in the micropores migrates onto nearby active CoMo sites in the mesopores, which could be responsible for the great enhancement of the HDS activity (Tang et al. 2013). These features are crucial for the design and preparation of multifunctional high activity catalysts for HDS, selective cracking, and hydrocracking (Tang et al. 2013). The alumina-nano Y zeolite (Al_2O_3-nY) composites reduce the metal-support interaction and heighten the MoS_2 stacking degree, shorten slabs, and enlarge corner Mo atoms. The addition of nanozeolite also enhances the overall acidity, which improves the HDS activity compared with $NiMo/Al_2O_3$ catalysts. Synergism of the hydrogenation activity and acid amounts is responsible for the improved activity (Yin et al. 2011, 2015). The differences in the basicity and/or acidity of support materials are important contributors to the performance of desulfurization catalyst (Zhang et al. 2015). A large amount of the strong basic sites can avoid the polymerization of catalyst species and form small oxide clusters. On Co-MoS_2/NS-MgO, after sulfidation, small MoS_2 clusters with shorter lengths and less stacking formed on the NS-MgO contribute to an increase in the sites available for Co-promotion, resulting in the Co-MoS_2/NS-MgO catalyst with a high HDS activity (Zhang et al. 2015).

3.4 Fisher–Tropsch Synthesis

Fischer–Tropsch synthesis (FTS) is one of the efficient ways to convert coal, biomass, and natural gas into hydrocarbon derivatives through the intermediacy of synthesis gas (a mixture of H_2 and CO) on supported metal catalysts (Jiao et al. 2016). The greatest challenge with this process in the production of olefins is low

conversion and selectivity to lighter olefins ($C_{2=}$ to $C_{4=}$). Towards overcoming these limitations, supported metal nanoparticles have shown high promise as an effective catalyst for increasing conversion of lower olefins (López and Corma 2012; Galvis et al. 2012). Conversion of syngas to C_2 through C_4 olefins with selectivity up to 60 w%, using catalysts that compose of iron nanoparticles, homogeneously dispersed on weakly interactive α-alumina or carbon nanofibers supports is reported (Galvis et al. 2012). The use of iron nanoparticles improves stability of the reaction performed at high temperature, which is necessary to shift product selectivity to lighter hydrocarbons that is lacking with bulk iron catalysts. At a high temperature, the undesirable Boudouard reaction, $2CO(g) \rightarrow C(s) + CO_2(g)$ (Steynberg and Dry 2004), leads to the deposition of carbon, which can block the active sites and induce fragmentation of the particles in bulk iron catalysts (Shroff et al. 1995). The mechanical and thermal instabilities of the bulk iron oxide catalysts also result in the plugging of the catalyst bed in fixed-bed operation or in the fouling of separation equipment in a fluidized-bed process (Galvis et al. 2012). Compared with bulk Fe, the nanoparticle Fe catalysts display improved catalytic performances under industrial relevant conditions as shown in Fig. 2.9. It is also very clear that the support type exhibits significant effects on the performance for nano-Fe catalyst. After an initial activation period, Fe/b-SiC, Fe/CNF, 25 wt%Fe/α-Al_2O_3, and Fe/γ-Al_2O_3 show stable catalytic activities for up to 60 h (Galvis et al. 2012). The stability maintained during this time fully complies with the requirements for the application of catalysts in fluidized-bed reactors relevant in industrial applications of the exothermic FTS to olefins process.

The supported and bulk Fe catalysts tested in the FTS reaction at 1 bar and 350 °C at low CO conversion (0.5–1%) restrict secondary hydrogenation of olefins as shown in Table 2.1 (Galvis et al. 2012). Catalytic activity is expressed as iron time yield (i.e., the number of CO moles converted to hydrocarbons per gram of iron per second). A high initial activity is observed for Fe/b-SiC and Fe/CNF over 15 h. In Table 2.2, the activities and product selectivities measured after 64 h of reaction at 20 bar are displayed. The CO_2 selectivity for all the samples is approximately 40% on the basis of CO converted. The promoted catalysts prepared using supports with low interaction with iron show high catalytic activities combined with high selectivities to the desired products (Galvis et al. 2012).

Cobalt nanoparticles supported on mesoporous zeolites are effective catalysts for FTS (Cheng et al. 2015; Peng et al. 2015; Sartipi et al. 2014). The cooperative interplay of the Co sites and the acid sites on the zeolite forms a bifunctional catalyst that exhibits better performance than a monofunctional catalyst. A bifunctional catalyst consisting of uniform-sized Co nanoparticles and mesoporous H-ZSM-5 has been demonstrated to be effective for CO hydrogenation and hydrocracking/isomerization reactions (Cheng et al. 2015). The bifunctional catalyst was found to be promising for the direct production of gasoline-range (C_{5-11}) hydrocarbons from syngas. The Bronsted acidity in the zeolite results in hydrocracking/isomerization of the heavier hydrocarbons formed on Co nanoparticles, while the mesoporosity contributes to suppressing the formation of lighter (C_{1-4}) hydrocarbons. The selectivity for C_{5-11} hydrocarbons could reach about 70% with a ratio of

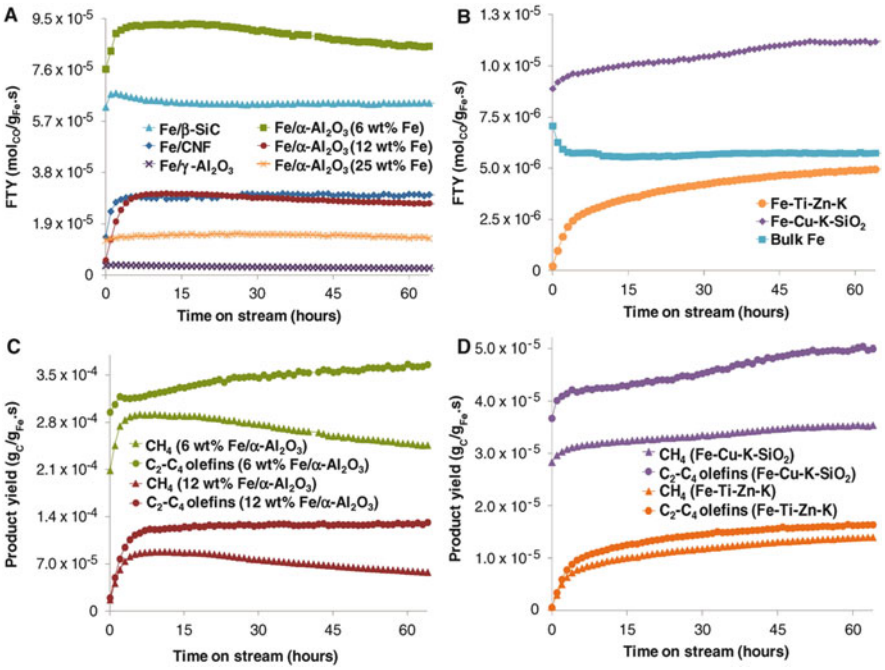

Fig. 2.9 (**a**–**d**) Catalytic performance of iron catalysts for the FTO process at 20 bar. Catalytic tests were carried out at $T = 340$ °C, $P = 20$ bar, and a H_2/CO ratio of 1. Iron time yield is plotted above as a function of time for (**a**) Fe-supported catalysts and (**b**) bulk Fe catalysts. Methane and lower olefins yields are plotted below as a function of time for (**c**) Fe-supported catalysts and (**d**) bulk Fe catalysts. The product yields were obtained at CO conversion levels between 70 and 80%. Adapted from Galvis et al. (2012). Reprinted with permission from The American Association for the Advancement of Science

isoparaffins to n-paraffins of approximately 2.3 over this catalyst, and the former is markedly higher than the maximum value (ca. 45%) expected from the Anderson–Schulz–Flory distribution (Cheng et al. 2015).

3.5 Other Reactions

Nanozeolite clinoptilolite supported rhodium nanoparticles (Rh/NZ-CP) were tested in the hydrogenation of arenes, nitroarenes, and alkenes under moderate reaction conditions. The nanocatalyst contains 2 wt% Rh of particle sizes in the range of 5–20 nm distributed on the zeolite. The catalytic performance of Rh/NZ-CP improves significantly, and the catalysts could be regenerated by a simple process and reused for many times without significant decrease in activity and selectivity. The high catalytic activity, thermal stability, and reusability present the

Table 2.1 Product selectivity and catalytic activity at 1 bar

Sample[a]	FTY (10^{-6} $mol_{co}/g_{Fe}.S$)	Selectivity (%C)			
		CH_4	C_2–C_4 Olefins	C_2–C_4 Paraffins	C_{5+}
Fe/CNF	1.41	23	61	4	12
Fe/α-Al_2O_3 (12 wt%Fe)	0.65	22	61	4	13
Fe/β-SiC	6.52	31	58	4	7
Fe/SiO_2	0.14	38	56	5	1
Fe/γ-Al_2O_3	0.07	54	44	2	0
Fe-Ti-Zn-K	0.13	83	16	1	0
Fe-Cu-K-SiO_2	0.20	43	46	2	9
Bulk Fe	0.08	76	21	2	1

From Galvis et al. (2012). Reprinted with permission from The American Association for the Advancement of Science

[a]Catalytic tests were performed at 350°C and an H_2/CO ratio of 1; results after 15 h on stream are shown (CO conversion: 0.5–1.0%). The product mixture that was analyzed consisted of C_1–C_{16} hydrocarbons. Iron time yield (FTY) represents moles of CO converted to hydrocarbons per mol of Fe per second; %C is defined as carbon atoms in a product with respect to the total number of C atoms in the hydrocarbon mixture

Table 2.2 Catalytic performance at 20 bar

Sample[a]	FTY (10^{-5} $mol_{co}/g_{Fe}.S$)	Selectivity (%C)				
		CH_4	C_2–C_4 olefins	C_2–C_4 paraffins	C_{5+}	Oxygenates
Fe/CNF	2.98	13	52	12	18	5
Fe/α-Al_2O_3 (6 wt%Fe)	8.48	24	35	21	10	10
Fe/α-Al_2O_3 (12 wt%Fe)	2.66	17	39	19	14	11
Fe/α-Al_2O_3 (25 wt%Fe)	1.35	11	53	6	21	9
Fe/β-SiC	6.38	35	19	39	4	3
Fe/γ-Al_2O_3	0.25	49	33	11	1	6
Fe-Ti-Zn-K	0.49	24	28	29	10	9
Fe-Cu-K-SiO_2	1.12	26	36	12	18	8
Bulk Fe	0.57	30	32	18	14	6

From Galvis et al. (2012). Reprinted with permission from The American Association for the Advancement of Science

[a]Catalytic tests were performed at 340°C and a H_2/CO ratio of 1; results after 64 h on stream are shown. The product mixture that was analyzed consisted of C_1 to C_{10} hydrocarbons

catalyst as an attractive option when compared with the conventional (Baghbanian et al. 2015).

The catalytic cracking of *n*-hexane over nano-ZSM-5 zeolite (MFI-type zeolite, Si/Al = 150 and 240) catalysts was tested at reaction temperatures ranging from 823 to 923 K under atmospheric pressure (Konno et al. 2012). The catalysts, compared with the micron-sized zeolite, exhibited a higher *n*-hexane conversion

with stable activity up to 50 h (Table 2.3). The Thiele modulus and the effectiveness factors for the reaction using ZSM-5 zeolites with different crystal sizes are presented in Fig. 2.10 and Table 2.4. It can be clearly seen from Table 2.4 that the effectiveness factor for MFI (S)150, that is, small crystallite size MFI with Si/Al of 150 is 1.0, indicating that the catalytic reaction in MFI(S)150 proceeded under reaction-controlled conditions (Konno et al. 2012). The large external surface area and low diffusion resistance of the nanozeolites reduce the effect of pore plugging due to coke deposition (Yin et al. 2014). For this reason, the application of nanozeolite in the catalytic cracking of *n*-hexane is effective in stabilizing the catalytic activity. Similarly, in the cracking of *n*-hexane and naphthenes, (cyclohexane and methyl-cyclohexane), coke was readily formed from the beginning of the reaction leading to significant deactivation of the catalyst for micron-sized ZSM-5 (Konno et al. 2013). For ZSM-5 catalysts, regardless of the reactant, the nanoscale ZSM-5 exhibited a high conversion and a high light olefins yield with a stable activity. As a result, the application of nanoscale ZSM-5 zeolites to the catalytic cracking of naphtha is effective and gives light olefins with high yield and excellent stable activity. Nanosized β-zeolites for the isomerization of hexane are also active with good selectivity to branched isomers because of the high external surface area of the small particles of the nanosized β-zeolites and the rapid diffusion of the reactants and products (Sakthivel et al. 2009).

In another report, methanol conversion to light olefins was investigated over SAPO-34 nanocatalyst with a crystal size of about 50 nm, and its catalytic properties were compared with those of 600 nm SAPO-34 catalyst (Askari et al. 2012). The product distribution over the two catalysts was almost the same, but their deactivation behaviors differ considerably. SAPO-34 catalyst with large crystal deactivates faster than SAPO-34 nanocatalyst. This variation in the deactivation of the different SAPO-34 crystallites is attributed to the number of accessible cavities near their external surface and the diffusion limitation of the reactant and product molecules. Due to a shorter diffusion length, the residence time of the produced hydrocarbons is short, resulting in the long catalyst lifetime of the SAPO-34 nanocrystals. Incorporation of a stabilizer into active catalysts could influence their performance. Boron incorporation into H-ZSM-5 nanocatalyst results in the isomorphic substitution of B into the framework of H-ZSM-5 (Yaripour et al. 2015). The interaction between B species and H-ZSM-5 reduces the strong acid sites and generates new weak acid sites which modify the densities and distributions of acid sites on the [B]-HZSM-5. This raises the lifetime of the modified zeolite in MTO reaction up to 1300 h compared to that of the conventional reference sample 340 h (Yaripour et al. 2015). However, propylene selectivity does not change significantly with the substitution of B in H-ZSM-5. The deactivated catalysts reveal that incorporation of boron improves coke resistance of the ZSM-5 nanocatalyst. The considerable enhancements of the lifetime and catalytic stability are attributed to the reduction of strong/mild acid sites ratio as well as small crystal size of the [B]-H-ZSM-5 nanocatalyst. In summary, the boron-modified ZSM-5 nanocatalyst exhibits more stable catalytic performance and longer catalytic lifetime for the MTO reaction.

Table 2.3 *n*-Hexane conversion, product yields, and coke amounts over the catalyst with different crystallite sizes

Catalyst	Time (h)	Conversion (C-mol%)	Light olefins yield (C-mol%)				BTX yield (C-mol%)	Others yield (C-mol%)	Coke amount of after 50 h (wt.%)
			C2=	C3=	C4=	Total olefin			
MFI(S)150	0.5	94.1	20.8	32.7	3.8	57.3	4.2	32.6	
7	93.5	19.1	32.8	4	55.9	4.1	33.5	–	
50	82	13.2	29	4.7	46.9	4.5	30.6	59.6	59.1
MFI(M)150	0.33	92.2	22.8	30.3	6.6	59.7	4.3	28.2	
7.5	93.1	20.8	32.4	7.3	60.5	3.9	28.7	–	
50	81	13.6	31.3	8.4	53.3	2.6	25.1	21	21.0
MFI(L)150	0.33	94.7	23.9	28.6	5.9	58.4	6.2	30.1	
8.5	81	13.6	30.8	8.1	52.5	3.1	25.4	–	
50	48.3	6.2	19.5	6.3	32	1.5	14.8	7.5	7.5

Reprinted from Konno et al. (2012) with permission from Elsevier. Copyright 2012, Elsevier publishers

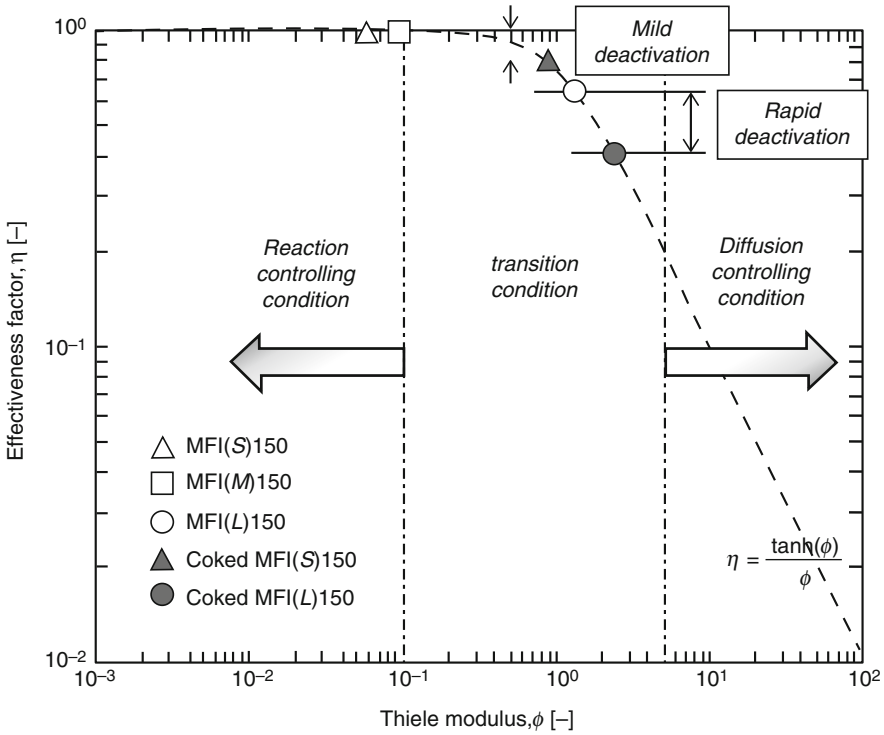

Fig. 2.10 Relationship between the Thiele modulus and the effectiveness factor in *n*-hexane cracking at 923 K over ZSM-5 zeolites (Si/Al = 150) with different crystal sizes. Adapted from Konno et al. (2012) with permission from Elsevier. Copyright 2012 Elsevier publishers

Table 2.4 Effectiveness factors of ZSM-5 zeolites (Si/Al = 150) with different crystal sizes in *n*-hexane cracking at 923 K

Sample	Reaction rate constant k ($m^3\ kg^{-1}\ s^{-1}$)	Thiele modulus ϕg (mc)	Effectiveness factor ηg (mc)
MFI(S)150	(1.04) 150^{-2}	(5.38) 150^{-2}	1
MFI(M)150	–	(8.97) 150^{-2a}	1
MFI(L)150	–	1.38[a]	0.65
Coked MFI(S) 150	8.27 MFI^{-3}	9.03 MFI^{-1}	0.8
Coked MFI(L) 150	4.24 MFI^{-3}	2.41	0.41

Reprinted from Konno et al. (2012) with permission from Elsevier. Copyright 2012, Elsevier publishers

[a]Theoretical value calculated from reaction rate constant of MFI(S)150

4 Concluding Notes and Future Perspectives

The relationship between nanoscience/nanotechnology and catalysis offers huge opportunities for improvements in petroleum processing. The utilization of nanoporous materials as supports and as active catalysts and metal nanoparticles for catalysis traverses various petroleum refining processes. The tremendous benefits the nanoscale materials possess over their micron-sized counterparts are due to their intrinsic size-dependent properties. The formulation of ideal nanoparticles to improve a process efficiency requires careful designed and controlled experiments. The improvements of several features make them a better choice. The properties that make them ideal candidates for petroleum processing include a greater surface area to volume ratio due to tiny particle size, and thermal and catalytic stability. Although the physiochemical characteristics of nanoparticles, such as phase, structure, or behavior, may be influenced by the method of preparation and the nature of the environment in which the nanoparticles are subjected to, the extent of these factors on the particle properties can also be size dependent and therefore can be controlled. Phase transformation in a metal nanoparticle catalyst could lead to the catalyst deactivation. However, it is not true in the case of nanoporous materials such as zeolites. The large external surface area to volume ratio decreases the tendencies of coke formation, which causes catalyst deactivation. Metal catalysts or solid acidic catalysts (such as zeolite) are utilized extensively in the petroleum industry, for example, in catalytic cracking hydrocracking, hydrodesulfurization, isomerization, reforming, and dehydrogenation.

The desire for improved catalysts with high activity, low deactivation, and low coke formation to increase production to meet the growing demand for chemicals and fuels are increasingly necessitating the exploitation of nanoparticles as catalysts, and there are even more opportunities lying to be explored using the potentials of nanotechnology. The inherent stability of nanoparticle catalysts and their bifunctional catalysis potentials provide even more future opportunities for many applications, such as the catalytic application to renewable fuels. Nanotechnology will continue to improve the future of petroleum refining explorations and exploitations. It is expected that lower energy consumption, extended lifetime of catalyst system and reduced amount of materials and reuse of nanomaterials will offer more environmentally friendly catalysts in the future.

References

Askari S, Halladj R, Sohrabi M (2012) Methanol conversion to light olefins over sonochemically prepared SAPO-34 nanocatalyst. Micropor Mesopor Mater 163:334–342

Askari S, Alipour SM, Halladj R, Farahani MHDA (2013) Effects of ultrasound on the synthesis of zeolites: a review. J Porous Mater 20:285–302

Baghbanian SM, Farhang M, Vahdat SM, Tajbakhsh M (2015) Hydrogenation of arenes, nitroarenes, and alkenes catalyzed by rhodium nanoparticles supported on natural nanozeolite clinoptilolite. J Mol Catal A Chem 407:128–136

Bell AT (2003) The impact of nanoscience on heterogeneous catalysis. Science 299:1688–1691

Besenbacher F, Chorkendorff I, Clausen B, Hammer B, Molenbroek A, Nørskov JK, Stensgaard I (1998) Design of a surface alloy catalyst for steam reforming. Science 279:1913–1915

Bezemer GL, Bitter JH, Kuipers HP, Oosterbeek H, Holewijn JE, Xu X, Kapteijn F, van Dillen AJ, de Jong KP (2006) Cobalt particle size effects in the Fischer-Tropsch reaction studied with carbon nanofiber supported catalysts. J Am Chem Soc 128:3956–3964

Busca G (2014) Metal oxides as acid-base catalytic materials. Elsevier, Amsterdam

Cheng K, Zhang L, Kang J, Peng X, Zhang Q, Wang Y (2015) Selective transformation of syngas into gasoline-range hydrocarbons over mesoporous H-ZSM-5-supported cobalt nanoparticles. Chem Eur J 21:1928–1937

Corma A, Lopez-Nieto J, Paredes N, Perez M, Shen Y, Cao H, Suib S (1992) Oxidative dehydrogenation of propane over supported-vanadium oxide catalysts. Stud Surf Sci Catal 72:213–220

Covarrubias C, Quijada R, Rojas R (2009) Synthesis of nanosized ZSM-2 zeolite with potential acid catalytic properties. Micropor Mesopor Mater 117:118–125

Database of Zeolite Structures. http://www.iza-structure.org/databases/

Davis ME, García-Martínez J, Li K (2015) Mesoporous zeolites: preparation, characterization and applications. Wiley, Weinheim

Farcasiu M, Degnan TF (1988) The role of external surface activity in the effectiveness of zeolites. Ind Eng Chem Res 27:45–47

Galvis HMT, Bitter JH, Khare CB, Ruitenbeek M, Dugulan AI, de Jong KP (2012) Supported iron nanoparticles as catalysts for sustainable production of lower olefins. Science 335:835–838

Gao Y, Wu G, Ma F, Liu C, Jiang F, Wang Y, Wang A (2016) Modified seeding method for preparing hierarchical nanocrystalline ZSM-5 catalysts for methanol aromatisation. Micropor Mesopor Mater 226:251–259

Grunes J, Zhu J, Somorjai GA (2003) Catalysis and nanoscience. Chem Commun 9 (18):2257–2260

Guo K, Gu M, Yu Z (2017) Carbon nanocatalysts for aquathermolysis of heavy crude oil: insights into thiophene hydrodesulfurization. Energy Technol. doi:10.1002/ente.201600522

Haruta M, Daté M (2001) Advances in the catalysis of Au nanoparticles. Appl Catal A Gen 222:427–437

Hauser JL, Tran DT, Conley ET, Saunders JM, Bustillo KC, Oliver SR (2016) Plasma treatment of silver impregnated mesoporous aluminosilicate nanoparticles for adsorptive desulfurization. Chem Mater 28:474–479

Hirota Y, Murata K, Miyamoto M, Egashira Y, Nishiyama N (2010) Light olefins synthesis from methanol and dimethylether over SAPO-34 nanocrystals. Catal Lett 140:22–26

Hu Y, Liu C, Zhang Y, Ren N, Tang Y (2009) Microwave-assisted hydrothermal synthesis of nanozeolites with controllable size. Micropor Mesopor Mater 119:306–314

Inayat A, Knoke I, Spiecker E, Schwieger W (2012) Assemblies of mesoporous FAU-type zeolite nanosheets. Angew Chem Int Ed 51:1962–1965

Jacobsen CJ, Madsen C, Houzvicka J, Schmidt I, Carlsson A (2000a) Mesoporous zeolite single crystals. J Am Chem Soc 122:7116–7117

Jacobsen CJ, Madsen C, Janssens TV, Jakobsen HJ, Skibsted J (2000b) Zeolites by confined space synthesis—characterization of the acid sites in nanosized ZSM-5 by ammonia desorption and ^{27}Al/^{29}Si-MAS NMR spectroscopy. Micropor Mesopor Mater 39:393–401

Jiao F, Li J, Pan X, Xiao J, Li H, Ma H, Wei M, Pan Y, Zhou Z, Li M (2016) Selective conversion of syngas to light olefins. Science 351:1065–1068

Jo C, Jung J, Shin HS, Kim J, Ryoo R (2013) Capping with multivalent surfactants for zeolite nanocrystal synthesis. Angew Chem 125:10198–10201

Kamigaito O (1991) What can be improved by nanometer composites? J Jpn Soc Powder Powder Metall 38:315–321
Karakoulia SA, Triantafyllidis KS, Tsilomelekis G, Boghosian S, Lemonidou AA (2009) Propane oxidative dehydrogenation over vanadia catalysts supported on mesoporous silicas with varying pore structure and size. Catal Today 141:245–253
Khalil M, Lee RL, Liu N (2015) Hematite nanoparticles in aquathermolysis: a desulfurization study of thiophene. Fuel 145:214–220
Khodakov A, Yang J, Su S, Iglesia E, Bell AT (1998) Structure and properties of vanadium oxide-zirconia catalysts for propane oxidative dehydrogenation. J Catal 177:343–351
Khodakov A, Olthof B, Bell AT, Iglesia E (1999) Structure and catalytic properties of supported vanadium oxides: support effects on oxidative dehydrogenation reactions. J Catal 181:205–216
Konno H, Okamura T, Kawahara T, Nakasaka Y, Tago T, Masuda T (2012) Kinetics of n-hexane cracking over ZSM-5 zeolites—effect of crystal size on effectiveness factor and catalyst lifetime. Chem Eng J 207:490–496
Konno H, Tago T, Nakasaka Y, Ohnaka R, J-i N, Masuda T (2013) Effectiveness of nano-scale ZSM-5 zeolite and its deactivation mechanism on catalytic cracking of representative hydrocarbons of naphtha. Micropor Mesopor Mater 175:25–33
Kore R, Srivastava R, Satpati B (2014) ZSM-5 zeolite nanosheets with improved catalytic activity synthesized using a new class of structure-directing agents. Chem Eur J 20:11511–11521
Lei Y, Mehmood F, Lee S, Greeley J, Lee B, Seifert S, Winans RE, Elam JW, Meyer RJ, Redfern PC (2010) Increased silver activity for direct propylene epoxidation via subnanometer size effects. Science 328:224–228
Li YH, Zhu YQ (2012) Research progress of unsupported nano catalyst. Adv Mater Res 550–553:284–291. Trans Tech Publ
Li G, Jones CA, Grassian VH, Larsen SC (2005) Selective catalytic reduction of NO_2 with urea in nanocrystalline NaY zeolite. J Catal 234:401–413
Lindsay S (2009) Introduction to nanoscience. Oxford University Press, New York
López C, Corma A (2012) Supported iron nanoparticles as catalysts for sustainable production of lower olefins. ChemCatChem 4:751–752
Lv Y, Qian X, Tu B, Zhao D (2013) Generalized synthesis of core-shell structured nano-zeolite@ ordered mesoporous silica composites. Catal Today 204:2–7
McHale J, Auroux A, Perrotta A, Navrotsky A (1997) Surface energies and thermodynamic phase stability in nanocrystalline aluminas. Science 277:788–791
Mehlhorn D, Inayat A, Schwieger W, Valiullin R, Kärger J (2014) Probing mass transfer in mesoporous faujasite-type zeolite nanosheet assemblies. ChemPhysChem 15:1681–1686
Mintova S, Olson NH, Valtchev V, Bein T (1999) Mechanism of zeolite A nanocrystal growth from colloids at room temperature. Science 283:958–960
Mintova S, Grand J, Valtchev V (2016) Nanosized zeolites: Quo Vadis? C R Chim 19:183–191
Mohajeri A, Rashidi A, Jozani KJ, Khorami P, Amini B, Parviz D, Kalbasi M (2010) Hydrodesulphurization nanocatalyst, its use and a process for its production. U.S. Patent No. 20100167915
Mohammed MI, Razak AAA, Shehab MA (2017) Synthesis of nanocatalyst for hydrodesulfurization of gasoil using laboratory hydrothermal rig. Arab J Sci Eng 42 (4):1381–1387
Morales-Pacheco P, Domínguez J, Bucio L, Alvarez F, Sedran U, Falco M (2011) Synthesis of FAU (Y)-and MFI (ZSM5)-nanosized crystallites for catalytic cracking of 1, 3, 5-triisopropylbenzene. Catal Today 166:25–38
Ng E-P, Chateigner D, Bein T, Valtchev V, Mintova S (2012a) Capturing ultrasmall EMT zeolite from template-free systems. Science 335:70–73
Ng E-P, Goupil J-M, Al V, Fernandez C, Retoux R, Valtchev V, Mintova S (2012b) Nucleation and Crystal Growth Features of EMT-Type Zeolite Synthesized from an Organic-Template-Free System. Chem Mater 24:4758–4765

Pan Y, Ju M, Yao J, Zhang L, Xu N (2009) Preparation of uniform nano-sized zeolite A crystals in microstructured reactors using manipulated organic template-free synthesis solutions. Chem Commun 7233–7235. doi: 10.1039/b917949f

Park HJ, Jeon J-K, Kim JM, Lee HI, Yim J-H, Park J, Park Y-K (2008) Synthesis of nanoporous material from zeolite USY and catalytic application to bio-oil conversion. J Nanosci Nanotechnol 8:5439–5444

Peng X, Cheng K, Kang J, Gu B, Yu X, Zhang Q, Wang Y (2015) Impact of hydrogenolysis on the selectivity of the Fischer-Tropsch synthesis: diesel fuel production over mesoporous zeolite-Y-supported cobalt nanoparticles. Angew Chem 127:4636–4639

Persson AE, Schoeman BJ, Sterte J, Otterstedt JE (1994) The synthesis of discrete colloidal particles of TPA-silicalite-1. Zeolites 14:557–567

Rafiee E, Rezaei S (2016) Deep extractive desulfurization and denitrogenation of various model oils by $H_{3+n}PMo_{12-n}V_nO_{40}$ supported on silica-encapsulated γ-Fe_2O_3 nanoparticles for industrial effluents applications. J Taiwan Inst Chem Eng 61:174–180

Rajagopalan K, Peters AW, Edwards GC (1986) Influence of zeolite particle size on selectivity during fluid catalytic cracking. Appl Catal 23:69–80

Rao C, Kulkarni G, Thomas PJ, Edwards PP (2002) Size-dependent chemistry: properties of nanocrystals. Chem Eur J 8:28–35

Rezvani MA, Shojaei AF, Zonoz FM (2014) Anatase titania–vanadium polyphosphomolybdate as an efficient and reusable nano catalyst for the desulphurization of gas oil. J Serb Chem Soc 79:1099–1110

Sakthivel A, Iida A, Komura K, Sugi Y, Chary KV (2009) Nanosized β-zeolites with tunable particle sizes: synthesis by the dry gel conversion (DGC) method in the presence of surfactants, characterization and catalytic properties. Micropor Mesopor Mater 119:322–330

Sartipi S, Alberts M, Santos VP, Nasalevich M, Gascon J, Kapteijn F (2014) Insights into the catalytic performance of mesoporous H-ZSM-5-supported cobalt in Fischer-Tropsch synthesis. ChemCatChem 6:142–151

Schlögl R, Abd Hamid SB (2004) Nanocatalysis: mature science revisited or something really new? Angew Chem Int Ed 43:1628–1637

Schmidt I, Madsen C, Jacobsen CJ (2000) Confined space synthesis. A novel route to nanosized zeolites. Inorg Chem 39:2279–2283

Schoeman B, Sterte J, Otterstedt J-E (1994) Colloidal zeolite suspensions. Zeolites 14:110–116

Serrano DP, van Grieken R, Melero JA, García A, Vargas C (2010) Nanocrystalline ZSM-5: a catalyst with high activity and selectivity for epoxide rearrangement reactions. J Mol Catal A Chem 318:68–74

Shroff MD, Kalakkad DS, Coulter KE, Kohler SD, Harrington MS, Jackson NB, Sault AG, Datye AK (1995) Activation of precipitated iron Fischer-Tropsch synthesis catalysts. J Catal 156:185–207

Steynberg A, Dry M (2004) Fischer-Tropsch technology. Elsevier, Amsterdam

Sudhakar C (1998) Selective hydrodesulfurization of cracked naphtha using novel catalysts. U.S Patent No. 5770046

Sun W, Wang L, Zhang X, Liu G (2015) Controllable synthesis of hierarchical beta nanozeolites from tailorable seeds. Micropor Mesopor Mater 201:219–227

Tang T, Zhang L, Fu W, Ma Y, Xu J, Jiang J, Fang G, Xiao F-S (2013) Design and synthesis of metal sulfide catalysts supported on zeolite nanofiber bundles with unprecedented hydrodesulfurization activities. J Am Chem Soc 135:11437–11440

Vajda S, Pellin MJ, Greeley JP, Marshall CL, Curtiss LA, Ballentine GA, Elam JW, Catillon-Mucherie S, Redfern PC, Mehmood F, Zapol P (2009) Subnanometre platinum clusters as highly active and selective catalysts for the oxidative dehydrogenation of propane. Nat Mater 8:213–216

Valden M, Lai X, Goodman DW (1998) Onset of catalytic activity of gold clusters on titania with the appearance of nonmetallic properties. Science 281:1647–1650

Valtchev V, Tosheva L (2013) Porous nanosized particles: preparation, properties, and applications. Chem Rev 113:6734–6760

Vuong G-T, Hoang V-T, Nguyen D-T, Do T-O (2010) Synthesis of nanozeolites and nanozeolite-based FCC catalysts, and their catalytic activity in gas oil cracking reaction. Appl Catal A Gen 382:231–239

Wachs IE, Weckhuysen BM (1997) Structure and reactivity of surface vanadium oxide species on oxide supports. Appl Catal A Gen 157:67–90

Weisz PB (1995) Molecular diffusion in microporous materials: formalisms and mechanisms. Ind Eng Chem Res 34:2692–2699

Yang F, Deng D, Pan X, Fu Q, Bao X (2015) Understanding nano effects in catalysis. Natl Sci Rev 2:183–201

Yaripour F, Shariatinia Z, Sahebdelfar S, Irandoukht A (2015) Effect of boron incorporation on the structure, products selectivities and lifetime of H-ZSM-5 nanocatalyst designed for application in methanol-to-olefins (MTO) reaction. Micropor Mesopor Mater 203:41–53

Yin H, Zhou T, Liu Y, Chai Y, Liu C (2011) $NiMo/Al_2O_3$ catalyst containing nano-sized zeolite Y for deep hydrodesulfurization and hydrodenitrogenation of diesel. J Nat Gas Chem 20:441–448

Yin X, Chu N, Yang J, Wang J, Li Z (2014) Synthesis of the nanosized MCM-22 zeolite and its catalytic performance in methane dehydro-aromatization reaction. Catal Commun 43:218–222

Yin H, Liu X, Yao Y, Zhou T (2015) Nanosized HY zeolite-alumina composite support for hydrodesulfurization of FCC diesel. J Porous Mater 22:29–36

Yutthalekha T, Wattanakit C, Warakulwit C, Wannapakdee W, Rodponthukwaji K, Witoon T, Limtrakul J (2016) Hierarchical FAU-type zeolite nanosheets as green and sustainable catalysts for benzylation of toluene. J Clean Prod 142:1244–1251

Zhang YL, Jin XJ, Rong YH, Hsu TY, Jiang DY, Shi JL (2006) The size dependence of structural stability in nano-sized ZrO_2 particles. Mater Sci Eng A 438–440:399–402

Zhang H, Chen B, Banfield JF (2009) The size dependence of the surface free energy of titania nanocrystals. Phys Chem Chem Phys 11:2553–2558

Zhang L, Fu W, Xiang M, Wang W, He M, Tang T (2015) MgO Nanosheet assemblies supported CoMo catalyst with high activity in hydrodesulfurization of dibenzothiophene. Ind Eng Chem Res 54:5580–5588

Zheng N, Stucky GD (2006) A general synthetic strategy for oxide-supported metal nanoparticle catalysts. J Am Chem Soc 128:14278–14280

Zhou B (2007) Nanotechnology in catalysis volumes 3. Springer, New York

Zhou X, Xu W, Liu G, Panda D, Chen P (2009) Size-dependent catalytic activity and dynamics of gold nanoparticles at the single-molecule level. J Am Chem Soc 132:138–146